Structure of Glucagon-like Peptide(7–36) Amide in a Dodecylphosphocholine Micelle as Determined by 2D NMR†

Kevin Thornton and David G. Gorenstein*

Department of Chemistry, Purdue University, West Lafayette, Indiana 47907

Received October 18, 1993; Revised Manuscript Received January 10, 1994®

ABSTRACT: We have used 2D ^{1}H NMR to determine the structure of glucagon-like peptide-1-(7–36) amide bound to a dodecylphosphocholine micelle. In this membranelike environment, the peptide hormone is shown to have a structure similar to that observed for glucagon. It consists of an N-terminal random coil segment (residues 1–7), two helical segments (7–14 and 18–29), and a linker region (15–17). The C-terminal helix is more stable than the N-helix as determined by amide proton exchange experiments. The C-terminal helix shows much larger α and amide proton upfield secondary shifts relative to those expected for a random coil conformation. This suggests a highly helical structure in this portion of the molecule. The C-terminal helix also has a much larger fraction of residues that are hydrophobic, presumably enhancing the interaction of this portion of the peptide with the micelle (or membrane). The structure refined from the NOESY data is not a uniform α-helix throughout residues 6–30. A uniform helix would not be perfectly amphiphilic since the hydrophobic face of the N-terminal portion of the helix is positioned in nearly perfect opposition to the hydrophobic face of the C-terminal portion. However, helical distortion around residues 15–17 allows a phase shift of the two helical segments to position nearly all of the hydrophobic residues (and none of the hydrophilic ones) on a single face of the distorted single helix as would be required to favorably interact with the hydrophobic portion of the micelle or membrane.

Glucagon-like peptide-1 (GLP-1) is an incretin found in the L-cells of the intestine or α-cells of the pancreas (Mojsov et al., 1990) of mammals (Gutniak et al., 1992; Mojsov et al., 1990; Ørskov et al., 1989). It is one of three products liberated upon processing of preproglucagon by intestinal L-cells (Mojsov et al., 1990; Thorens, 1992). Processing of preproglucagon produces the peptide fragments glycentin, GLP-1, and GLP-2. Both GLP-1 and GLP-2 sequences show 50% homology with that of glucagon. In fact, the GLP-1 sequence is highly conserved in mammals, showing 100% identity between the GLP-1 sections of proglucagon that have been studied (Ørskov et al., 1989).

GLP-1 has been shown to possess no biological activity in its nontruncated form. However, two truncated forms of GLP-1, GLP-1-(7–37) and GLP-1-(7–36)NH_2, have been shown to possess potent biological activity. Both GLP-1-(7–37) and GLP-1-(7–36)NH_2 exhibit identical effects. They have both been shown to strongly increase insulin secretion and reduce glucagon secretion (Thorens, 1992). GLP-1-(7–37) and GLP-1-(7–36)NH_2 have also been shown to lower the meal-related increase in blood glucose levels and the plasma concentrations of glucose and insulin (Gutniak et al., 1992). GLP-1-(7–36)NH_2 is of interest because of its "antidiabetogentic" effects. It is thought that GLP-1-(7–36)NH_2 could be an important tool in the treatment of non-insulin-dependent diabetes mellitus (Gutnaik et al., 1992; Thorens & Waeber, 1993). GLP-1-(7–37) and GLP-1-(7–36)NH_2 have been shown to act by binding to a receptor located on the surface of pancreas β-cells (Thorens, 1992).

In this paper, we report the NMR structure of the GLP-1-(7–36)NH_2 peptide in a membranelike environment (a dodecylphosphocholine micelle). An important caveat must always be raised whether the conformation of a peptide, even on the surface of the membrane (let alone micelle), has any relevance to our understanding of the conformational features of the peptide that are recognized in the receptor-bound state. In purely aqueous solution, these short peptides are largely random coils. However, in the membranelike environment of the micelle, these peptides form a stable secondary structure. We hope to show that these latter structures provide potentially important information with which we may interpret biological function. Combined with the recent isolation of the GLP-1 receptor, it may ultimately prove possible to design new analogues of GLP-1 in the treatment of non-insulin-dependent diabetes mellitus.

MATERIALS AND METHODS

Peptide Synthesis and Purification. The solid-phase synthesis of GLP-1-(7–36) amide was carried out on a Model 430A peptide synthesizer (Applied Biosystems, Foster City, CA) using the Boc protecting strategy. The side-chain protecting groups used were Asp (Chxl), Glu (OBzl), Ser (Bzl), Thr (Bzl), Lys (Cl-z), His (BOM), Trp (CHO), Tyr (Br-Z), and Arg (Tos). All except for Asp (Chxl) (Peptides International) were obtained from Applied Biosystems. A *p*-methylbenzhydrylamine resin (0.66 mm/g, Applied Biosystems) was used, and each residue was double coupled. The N-terminal Boc group was removed from the completed peptidyl resin via an "end-NH_2" cycle. The Trp (CHO) was removed by a 20% piperidine in DMF treatment at 4 °C for 1 h. The peptidyl resin was washed several times with CH_2Cl_2, transferred to a Teflon reaction vessel, and dried in vacuo to give 2.36 g; 1-mL of *m*-cresol and a magnetic stir bar were added. The vessel was attached to an HF apparatus (Pennisula Laboratories, Inc.), cooled to −78 °C, and evacuated, and 14 mL of HF was condensed in. The reaction mixture was stirred for 60 min in an ice bath and then the HF was removed in

† Supported by NIH (AI27744), the Office of Naval Research (N00014-91-J-1686), and the Purdue University Biochemical Magnetic Resonance Laboratory, which is supported by the NIH designated AIDS Research Center at Purdue (AI727713) and the NSF designated Biological Facilities Center on Biomolecular NMR, Structure and Design at Purdue (Grants BBS 8614177 and 8714258 from the Division of Biological Instrumentation).

® Abstract published in *Advance ACS Abstracts,* March 1, 1994.

0006-2960/94/0433-3532$04.50/0

vacuo. The residue was suspended in ethyl ether (200 mL), and stirred briefly, and then the solid material was filtered using a 60-mL glass-fritted filter funnel. After the solids were washed twice with ether, the peptide was solubilized by washing the solids with 20-mL portions of 50% aqueous HOAc, 10% aqueous HOAc, and water. The aqueous filtrate was loaded onto a 2.2 × 25-cm Vydac C18 and preparatively chromatographed on a FPLC (Pharmacia). Fractions of 7 min were collected in a gradient of 40–100% B over 1000 min at room temperature, 280 nm (A = 0.1% TFA; B = 0.1% TFA/50% CH_3CN). Analytical HPLC analysis of various fractions led to the combination of fractions 61–74. On lyophilization, 121.5 mg was obtained. The product was characterized by electrospray mass spectroscopy, amino acid analysis, amino acid sequencing, and NMR (see below). The data were consistent with those of GLP-1-(7–36)NH_2.

NMR. The NMR sample was 7 mM GLP-1-(7–36)NH_2 and 283 mM deuterated dodecylphosphocholine (MSD Isotopes) in 0.6 mL of 50 mM NaP_i (90% H_2O/10% D_2O), pH 6.0 (uncorrected) (Braun et al., 1983; Bösch et al., 1980). All spectra were recorded at 37 °C on a Varian VXR 600 spectrometer operating at proton frequencies of 600 MHz. The sweep width was 7500-Hz for experiments used in making assignments. Spectra were referenced to an external sample of DSS in 90% H_2O/10% D_2O, pH 6.0 (uncorrected). Water suppression was accomplished by selective saturation of water during the relaxation delay of all NMR experiments as well as during the mixing period of the pure absorption-phase NOESY experiments. All 2D experiments used in making assignments were recorded with 16 transients, 1024 complex points in the $t1$ dimension, and 2048 points in the $t2$ dimension. Zero filling to 2K × 2K was performed on all experiments. A 90° or 45° sine-bell window function was applied to the NOESY FID prior to transforming in both dimensions. Mixing times of 50, 80, and 125 ms were used for NOESY spectra. TOCSY experiments (Bax & Davis, 1985; Braunschweiler & Ernst, 1983) were acquired with a 50- or 100-ms spin–lock period and processed using a cosine bell. A double-quantum-filtered COSY (Piantini et al., 1982; Rance et al., 1983) was processed with a sine-bell function prior to transformation. Data sets were processed on SUN 4 workstations utilizing VNMR software from Varian. NH exchange experiments were acquired using a TOCSY sequence with 8 transients, 256 complex points in $t1$, and 2048 points in $t2$ at pH 3.0 and 37 °C. Spectra were processed using a 90°-shifted sine bell and zero filled to 2K × 1K in $t2$ and $t1$, respectively.

Minimization and Molecular Dynamics. A model structure for the peptide was built on a Silicon Graphics Iris 4D25S workstation utilizing UCSF MIDAS Plus software (Langride & Ferrin, 1984). Minimization and molecular dynamics were performed using a modified version of AMBER 4 (Weiner & Kollman, 1981a) which contains a flatwell pseudopotential to constrain the peptide with the NOE distances (Nikonowicz et al., 1989). In addition, the peptide was built using pseudoatom residues (Wüthrich et al., 1983), as stereospecific assignments could not be made due to overlap in the spectra. A total of 110 interresidue distance constraints derived from peak volumes or intensities were obtained from a 50-ms NOESY spectrum at 37 °C. NOEs were categorized by their peak intensity as strong (>7, <3 Å), medium (2–7, <4 Å), or weak (<2, <5 Å) (Braun et al., 1983). An additional 0.5-Å correction factor was applied to distances involving methyl groups (Clore et al., 1987).

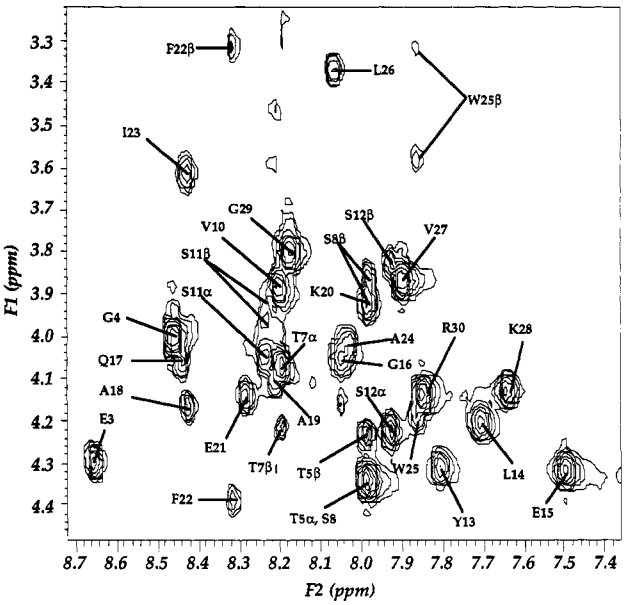

FIGURE 1: Fingerprint region showing the $C_\alpha H$–$N_\alpha H$ ^1H NMR cross peaks of the pure absorption-phase H_2O 2D TOCSY spectrum of GLP-1-(7–36)NH_2 peptide in a dodecylphosphocholine micelle solution, pH 6.0 (uncorrected) and 37 °C.

RESULTS

NMR Assignments. The ^1H NMR spectra of GLP-1-(7–36)NH_2 in a solution containing deuterated dodecylphosphocholine micelle were assigned through pure absorption-phase 2D NMR spectra in H_2O using standard methods (Wüthrich, 1986). We have used TOCSY (through bond), DQF-COSY (through bond), and NOESY (through space) NMR spectra in H_2O to identify spin systems of the different amino acid residues in the peptide. Portions of the pure absorption-phase H_2O TOCSY and NOESY spectra in the important "fingerprint" region are shown in Figures 1 and 2. After we identified the various spin systems, the sequentual connectivities across the peptide bond were assigned from NOESY spectra using standard sequential assignment methods (Wüthrich, 1986). The sequential assignments in the fingerprint region are diagrammed in Figure 2. When ambiguities occurred due to overlap in the spectrum, other regions of the NOESY spectra were used to resolve those ambiguities. The $C_\beta H_i$–$N_\alpha H_{i+1}$ (spectra not shown) and $N_\alpha H_i$–$N_\alpha H_{i+1}$ (Figure 3) cross peaks were particularly helpful in confirming the sequential assignments. The proton assignments are listed in Table 1.

Second, interresidue connectivities were identified from NOESY spectra. Most interresidue cross peaks used in the sequential assignments were taken from the fingerprint or NH–NH region of a 50-ms NOESY spectra. Figures 2 and 3 show the fingerprint and NH–NH region of the 50-ms NOESY spectrum.

Secondary Structure. The observed NOEs of GLP-1-(7–36)NH_2 are large and negative, indicating that the peptide is not in a random coil conformation in the micelle solution. In comparing the observed chemical shifts of the peptide with those predicted for a random coil (Wüthrich, 1986), we observe that the amide and α protons are shifted significantly upfield as shown in Figure 4A,B. Furthermore, the chemical shift differences between the α protons of GLP-1-(7–36)NH_2 and those expected for a random coil (Figure 4A) indicate the presence of two α-helical segments (Wishart et al., 1992). On the basis of the α proton chemical shifts, the two helical

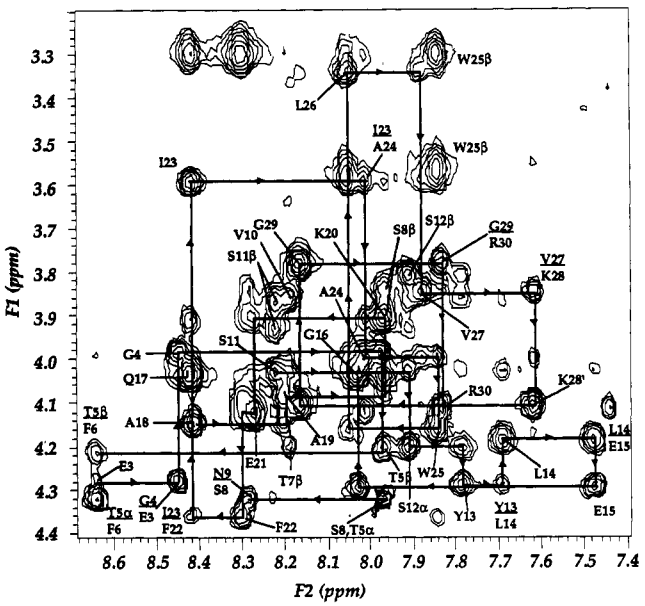

FIGURE 2: Fingerprint region showing the $C_\alpha H$–$N_\alpha H$ and $C_\alpha H_i$–$N_\alpha H_{i+1}$ ^1H NMR cross peaks of the pure absorption-phase H_2O 2D NOESY spectrum of GLP-1-(7–36)NH_2 peptide in a dodecylphosphocholine micelle solution, pH 6.0 (uncorrected) and 37 °C. The sequential $C_\alpha H_i$–$N_\alpha H_{i+1}$ connectivities and assignments are diagrammed.

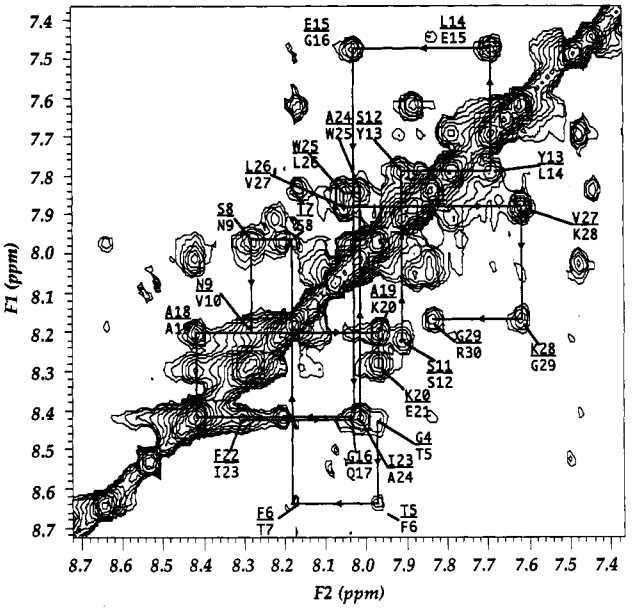

FIGURE 3: NH–NH region showing the $N_\alpha H_i$–$N_\alpha H_{i+1}$ ^1H NMR cross peaks of the pure absorption-phase H_2O 2D NOESY spectrum of GLP-1-(7–36)NH_2 peptide in a dodecylphosphocholine micelle solution, pH 6.0 (uncorrected) and 37 °C. The sequential $N_\alpha H_i$–$N_\alpha H_{i+1}$ connectivities and assignments are as diagrammed and are suggestive of α-helical character.

Table 1: Chemical Shifts of GLP-1-(7–36)NH_2 at 37 °C in a DPC Micelle

residue	amide	α	β	other
H1				
A2		4.34	1.37	
E3	8.66	4.31	2.06	γCH_2 2.29
G4	8.46	4.01		
T5	7.99	4.34	4.23	γCH_3 1.07
F6	8.65	*a*	3.15	
T7	8.19	4.07	4.22	γCH_3 1.18
S8	7.98	4.34	3.86, 3.91	
N9	8.30	*a*	2.70	
V10	8.20	3.88	2.11	γCH_3 0.88
S11	8.24	4.05	3.90, 3.95	
S12	7.93	4.23	3.83	
Y13	7.80	4.31	3.05	
L14	7.71	4.20	1.82, 1.63	γCH 1.82; δCH_3 0.84, 0.89
E15	7.50	4.32	1.99, 2.16	γCH_2 2.28, 2.37
G16	8.05	4.04		
Q17	8.44	4.06	2.11	γCH_2 2.40; NH_2 6.79, 7.66
A18	8.42	4.17	1.46	
A19	8.21	4.11	1.49	
K20	7.98	3.93	1.91, 1.96	γCH_2 1.42; δCH_2 1.66; ϵCH_2 2.97
E21	8.28	4.14	2.09, 2.18	γCH_2 2.35, 2.49
F22	8.31	4.39	3.32	$H_{2,6}$ 7.18
I23	8.43	3.61	2.03	γCH 1.35, 1.88; γCH_3 0.95; δCH_3 0.91
A24	8.03	4.02	1.52	
W25	7.86	4.18	3.32, 3.58	H_2 7.32; H_3 10.43; H_4 7.50; H_5 7.09; H_6 6.87; H_7 7.29
L26	8.07	3.36	1.66, 1.47	γCH 1.56; δCH_3 0.74;
V27	7.90	3.87	2.21	γCH_3 0.90, 0.98
K28	7.64	4.13	1.80, 1.88	γCH_2 1.41, 1.47; δCH_2 1.65; ϵCH_2 2.94
G29	8.17	3.80		
R30	7.84	4.14	1.70, 1.81	γCH_2 1.53; δCH_2 3.07; NH 7.47

[a] Chemical shift coincident with that of water.

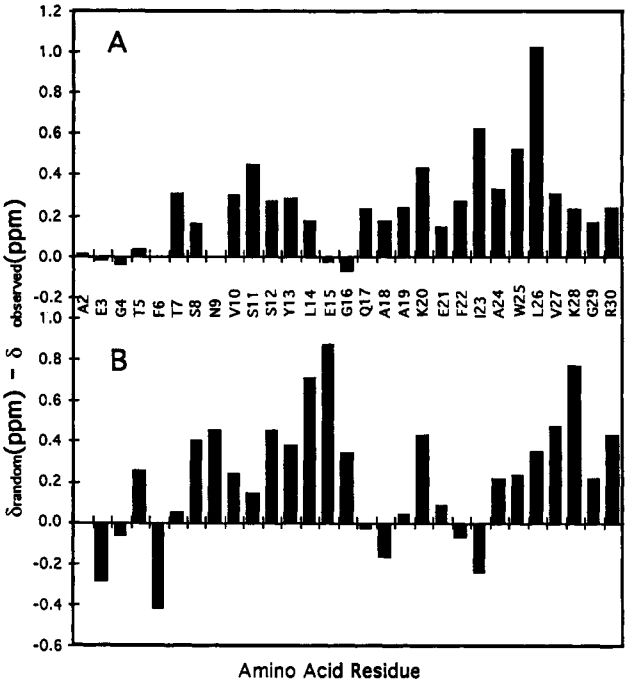

FIGURE 4: Difference between the ^1H NMR chemical shifts of the GLP-1-(7–36)NH_2 peptide in deuterated dodecylphosphocholine micelle solution at 37 °C and the chemical shifts predicted for a random coil conformation plotted against sequence. Missing entries as listed in Table 1 are represented by a blank. Positive differences indicate an upfield shift from the chemical shifts predicted for a random coil conformation (Wüthrich, 1986).

segments extend from residue 7 through 14 and from 17 through 30. This is similar to that reported for glucagon by Wüthrich and co-workers, where they observed two helical regions (10–14 and 17–29) (Wüthrich et al., 1983).

That there are two α-helical segments is further supported by the pattern of cross peaks observed in the NOESY spectra. The presence of $C_\alpha H_i$–$N_\alpha H_{i+2}$, $C_\alpha H_i$–$N_\alpha H_{i+3}$, $C_\alpha H_i$–$N_\alpha H_{i+4}$, and $C_\alpha H_i$–$C_\beta H_{i+3}$ cross peaks is strongly indicative of extensive α-helical structure (Wüthrich, 1986). These cross peaks are not observed in β-sheets. As shown in Figure 5, a number of these cross peaks are observed. These cross peaks confirm a high degree of α-helical structure from residues 8 through 30 with a break in the α-helical structure between residues 15

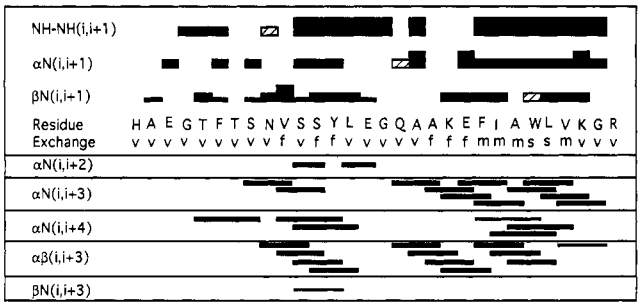

FIGURE 5: Amino acid sequence and medium-range sequential NOE connectivities from a 50-ms NOESY spectrum of GLP-1-(7–36)-NH_2 and Amino acid sequence and sequential NOE connectivities taken from a 50-ms NOESY at 37 °C for GLP-1-(7–36)NH_2 peptide in a dodecylphosphocholine micelle solution. Size of the solid boxes indicates peak volume. Boxes which are not solid were not quantitated.

and 17. Furthermore, as summarized in Figure 5, several $C_\beta H_i$–$N_\alpha H_{i+1}$ connectivities were also observed. These cross peaks have been shown to be more intense in α-helical regions (Hahn & Rüterjans, 1985).

Amide Exchange Kinetics. NH exchange experiments of GLP-1-(7–36)NH_2 in D_2O showed that while most amide protons exchanged within the first 22 min, a few were still present even after 1 day. Exchange rates were determined by a series of nine time-dependent 2D TOCSY experiments performed at pH 3.0 (uncorrected), and 37 °C. The fingerprint region showing assignments of remaining unexchanged cross peaks is shown in Figure 6. Each TOCSY experiment lasted 139 min and is identified in the figure by its starting time in minutes.

The 22-min TOCSY exhibited cross peaks to the amide protons for the amino acid residues V10, S12, Y13, A19, K20, E21, F22, I23, A24, W25, L26, and V27. However, by the 161-min TOCSY, amide protons from the N-terminal helix (V10, S12, Y13) and A19 had disappeared. By the 301-min TOCSY, the proton for E21 had disappeared. The amide proton of F22 had exchanged by 438 min and that of K20 by 715 min. Amide residues for I23, A24, W25, L26, and V27 (weak) were still present in the 1130-min TOCSY. Amide protons for W25 and L26 are still present after 24 h.

These results indicate that the hydrophobic residues (especially those on the C-terminal portion of the helix) are most protected from exchange. This can be explained by their being buried in the micelle and/or additional stabilization of this portion of the α-helix in the peptide/micelle complex. Analysis of a helical wheel representation of GLP-1-(7–36)-NH_2 is revealing. As shown in Figure 7, GLP-1-(7–36)NH_2 has two amphiphilic helical segments, each with a hydrophobic patch. The location of these amphiphilic helices is in each of the two α-helical segments identified from the NMR data.

DISCUSSION

NMR. GLP-1-(7–36)NH_2 shows 50% homology with that of glucagon. As shown in Figure 8, there is a significant degree of conservation between the two sequences. Residues 1, 4–8, 11, 13, 14, 19, 22, 25, and 26 are conserved in both sequences. Mutations at 10, 15, and 21 are conservative mutations. On the basis of the similarity of the sequences between GLP-1-(7–36)NH_2 and glucagon, it would be anticipated that the structure of these two peptides should also be similar.

NMR spectroscopy has the advantage over other biophysical probes of peptide conformation (such as CD spectroscopy) in that we can obtain information not only about the overall conformation of a peptide but also on local conformational structures and dynamics. By means of 2D NOESY experiments on GLP-1-(7–36)NH_2 bound to a micelle, we can readily distinguish segments of helical structure.

As shown in Figures 4 and 5, the NMR data of GLP-1-(7–36)NH_2 bound to a dodecylphosphocholine micelle are consistent with a structure made up of four regions. The first region extends from residue 1 through 6 and is primarily random coil. The second region extends from residue 7 through 14 and is α-helical. Region 3 is a short segment consisting of residues 15–17 and appears to be a loose helix. The fourth region is a second α-helical segment extending from residue 18 through 30.

These results are similar to those reported by Wüthrich and co-workers (Braun et al., 1983), wherein they have shown that glucagon bound to a dodecylphosphocholine micelle is random coil from residues 1 to 10, α-helical from residues 10 to 14, an extended chain from residues 14 to 17, and α-helical from residues 17 to 29. In the case of GLP-1-(7–36)NH_2, the helix located toward the N-terminal end is longer than that reported for glucagon (2.5 turns versus 1 turn). The secondary chemical shift patterns are also very similar. In both cases, residues 23 and 26 are shifted significantly upfield (see Figure 4).

Molecular Dynamics. Additional information about the solution structure and dynamics was obtained from NOESY distance-restrained molecular dynamics. We have utilized the NMR data and the molecular modeling program MIDAS (Langridge & Ferrin, 1984) to model build the structure of GLP-1-(7–36)NH_2 peptide, based upon the regions of secondary structure observed. Using the AMBER (Weiner & Kollman, 1981b) molecular mechanics/dynamics program, we first calculated a minimum-energy structure for the peptide consistent with the NOESY distance constraints. NOESY distance constraints (for the helix) were included as an additional flatwell pseudoenergy penalty term in the force field. Constraints were not violated by more than 0.1 Å.

After restrained molecular dynamics, the structure obtained showed extensive α-helical structure from residue 6 through 28. However, the ends of the peptide appear to be predominantly random coil (since, of course, only a few contraints were added to these residues) as shown in Figure 9. (These overlays are not intended to portray the relative accuracy or precision of the "refined" structure but to indicate the relative flexibility in various regions of the peptide. Without any tertiary NOE distance restraints, we can only define relatively accurately the local structure in the helical regions.) The variations in the individual structures also show that there is some flexibility around glycine 16, although there is some α-helixlike structure. The peptide segments consisting of residues 7–14 and 18–28 are highly helical. The average backbone rms error for the 10 structures calculated is 1.5 Å over residues 8–28, whereas that for the segments 8–16 or 16–28 is 0.70 and 0.79 Å, respectively.

A comparison of the backbone of the calculated solution structure of GLP-1-(7–36)NH_2 with the 3-Å resolution X-ray crystal structure of glucagon (Sasaki et al., 1975) shows significant similarity in the helical segments 7–14 and 18–28 of the peptide (rms fit for the peptide backbone of 1.0 and 1.3 Å for the segments 16–29 and 8–16, respectively). There is a much poorer rms fit (ca. 2.4 Å) of the entire helical region 8–29. However, because of the low resolution for both the NMR and X-ray structure, caution must be given to overly interpreting these differences.

Amide Exchange. Amide exchange rates can provide information about the relative stability and dynamics of the

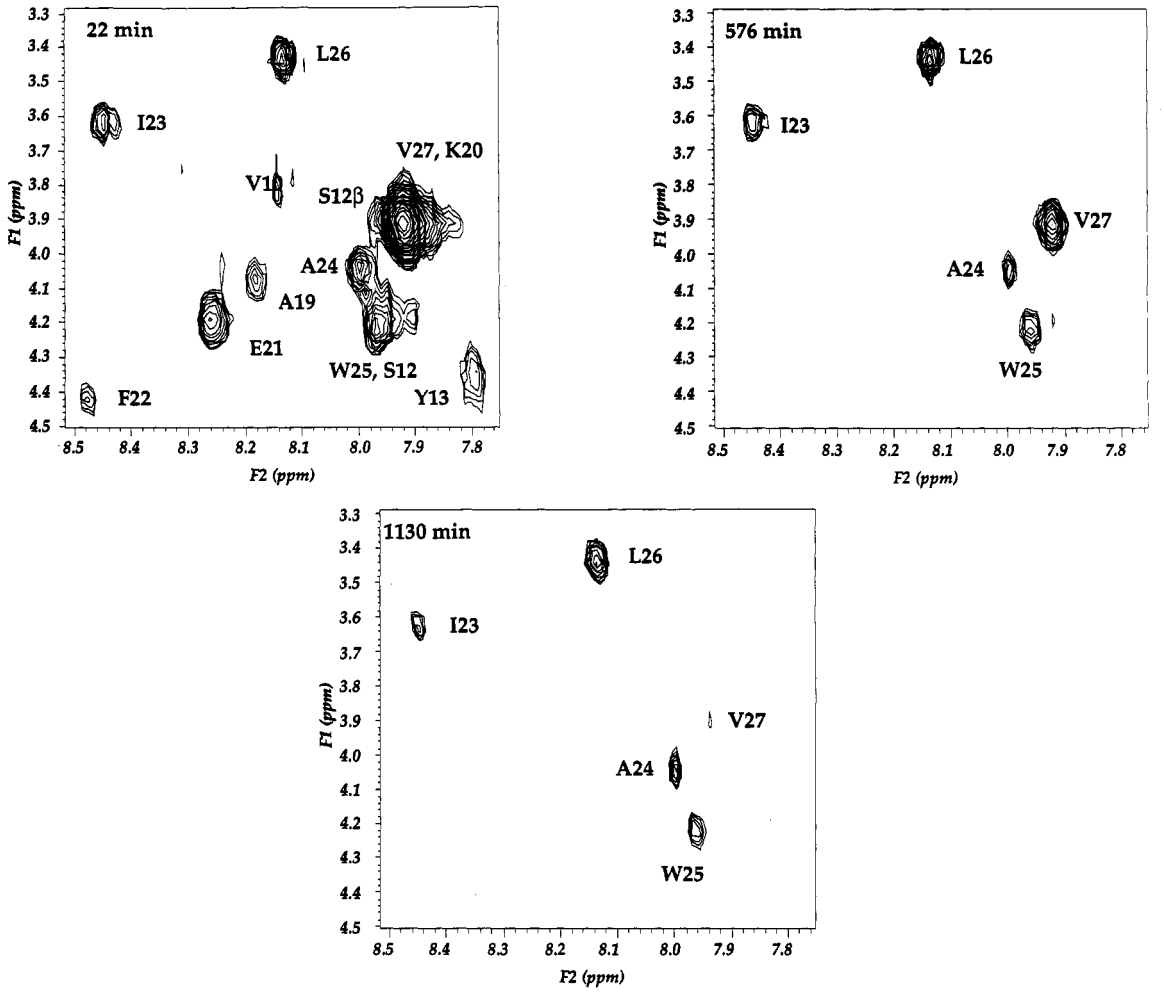

FIGURE 6: Fingerprint region of the pure absorption-phase TOCSY spectrum of GLP-1-(7–36)NH_2 peptide at 37 °C in dodecylphosphocholine micelle solution, pH 3.0, after addition of D_2O. Remaining $C_\alpha H_i$–$N_\alpha H_i$ cross peaks are labeled. Each TOCSY experiment lasted 139 min and is referred to by its starting time in minutes: (A, top left) 22-min NOESY, (B, top right) 576-min NOESY, and (C, bottom) 1130-min NOESY. Spectra are plotted with an identical vertical scale and threshold.

peptide secondary structure. In order for the amide protons of hydrophobic residues in a micelle-bound amphiphilic helix to exchange, it could require that hydroxide penetrate the hydrophobic interior of the micelle to exchange those amide hydrogens buried within the micelle. Alternatively, amide exchange could occur via local disruption of the helical portions of the GLP-1-(7–36)NH_2 peptide at either the surface or interior of the micelle or total dissociation of the peptide into the aqueous solution. If GLP-1-(7–36)NH_2 had little or no structure, NH exchange of the totally dissociated or random coil part of the partially dissociated peptide would be expected to be rapid.

The rate of exchange for a soluble globular protein that is predominantly in the folded state is given by

$$k_{ex} = K_{op}k_c$$

where k_c is the rate-limiting intrinsic rate of exchange of the unfolded protein and K_{op} the unfolding/folding equilibrium constant ($K_{op} = (k_u/k_f)$) (Englander & Kallenbach, 1984; Molday et al., 1972; Roder et al., 1985). This exchange-limited unfolding mechanism occurs under conditions where the folded state is stable and k_c is relatively slow. It has been shown by Sykes and co-workers (Henry et al., 1987a,b; Henry & Sykes, 1990) that the rate of amide proton exchange of the micelle-bound M13 coat protein can be interpreted in terms of this mechanism. These conditions most certainly apply for the micelle-bound GLP-1-(7–36)NH_2 peptide as well. Thus, the observed rate of exchange of the micelle-bound GLP-1-(7–36)NH_2 peptide will reflect both the intrinsic rate of exchange of the freely exposed amide to the solution as well as the fractional population of the locally unfolded state exposed to the solvent. Molday et al. (1972) [see also Roder et al. (1985)] have shown that most amide protons of random coil peptides exchange (k_c) within a relatively narrow range of values (generally less than 10-fold), depending upon the amino acid, nearest neighbor effects, and proximity to the N- and C-terminus.

Analysis of GLP-1-(7–36)NH_2 by the procedure of Molday allows us to predict the relative NH exchange rates expected for GLP-1-(7–36)NH_2 in a random coil (Molday et al., 1972). Amide exchange has generally been shown to be at a minimum at about pH 3.0 (Molday et al., 1972). The predicted order of base-catalyzed exchange is W25, A19, A24, V27 < F22, L14, K20, I23, L26, K28, E3, E15, A18 < F6, Y13, R30, Q17, E21, V10, S11 < G4, T7, G16 < N9, G29, T5, S8, S12, ≪ A2. There are clear differences between the predicted rates and those observed for micelle-bound GLP-1-(7–36)-NH_2. The observed order of exchange is L26 < W25, A24, I23 < F22 < V27(K20) < E21, A19, Y13, S12 < A2, E3, G4, T5, F6, T7, S8, N9, V10, S11, L14, E15, G16, Q17, A18, K28, G29, R30. Some amide protons of the GLP-1-(7–36)-NH_2 peptide remain even after 24 h, indicating that they are well sequestered from the solvent. It should be noted that shifts in the pH at which exchange is at a minimum (normally

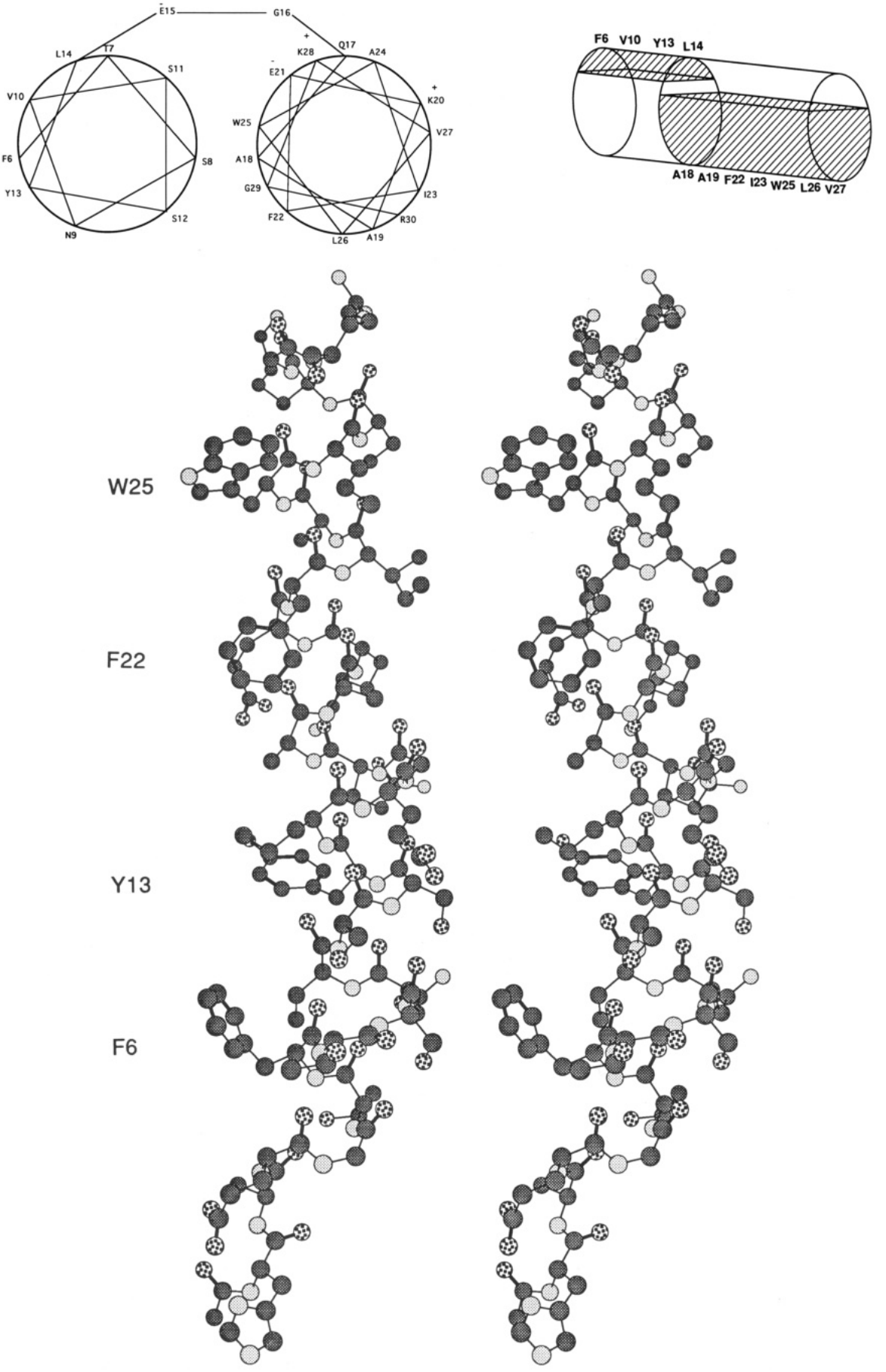

FIGURE 7: (A, top left) Helical wheel representation of the GLP-1-(7–36)NH_2 peptide as two separate amphiphilic helical segments. (B, top right) Schematic model of the glucagon helix derived from the X-ray crystal structure (Sasaki et al., 1975). Hydrophobic portions are shaded. (C, bottom) Stereoview of one of the final NOESY distance-restrained molecular dynamics structures of GLP-1-(7–36)NH_2 in a DPC micelle. NOESY distance-restrained molecular dynamics structures of GLP-1-(7–36)NH_2 in a DPC micelle.

FIGURE 8: Sequence comparison of GLP-1-(7–36)NH_2 and glucagon.

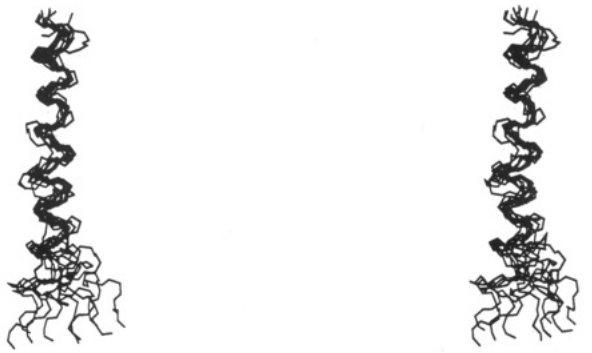

FIGURE 9: Stereoview overlay of final NOESY distance-restrained molecular dynamics structures of GLP-1-(7–36)NH_2 in a DPC micelle.

ca. pH 3.0) can also affect the relative exchange rates (Molday et al., 1972) and no correction has been made for this effect. The differential NH exchange rates are thus interpreted in terms of local unfolding of the peptide, exposing NH's to the solvent.

The NH exchange rates indicate that the C-terminal helix has a greater stability than the N-terminal helix. The C-terminal helical segment also shows much larger upfield shifts of the amide protons relative to those in a random coil conformation, again reflecting the enhanced helical stability of this portion of the molecule. As shown in Figure 7A, the C-terminal helix also has a much larger fraction of residues that are hydrophobic, presumably enhancing the interaction of this portion of the peptide with the micelle (or presumably the membrane in vivo). These results are in agreement with those reported by Wüthrich and co-workers, wherein they were able to show that even in dilute aqueous solution there is some residual structure in the C-terminal end between residues 22 and 26 (Bösch et al., 1980). This is also in agreement with Hruby and co-workers, where they have demonstrated that a stable C-terminal helix is essential for receptor binding of glucagon (Hruby et al., 1986).

Note that the structure calculated using NOE distance constraints is not a continuous α-helix from residues 6 through 30 as there is a break between residues 15 and 17 (see Figure 9). A continuous helix could not be perfectly amphiphilic as indicated by the schematic model of a perfect α-helix, Figure 7B. Thus, in a uniform helix, the hydrophobic face of the N-terminal portion of the helix (residues F6, V10, Y13, and L14) is positioned in nearly perfect opposition to the hydrophobic face of the C-terminal portion of the helix (residues A18, A19, F22, I23, W25, L26, and V27—shown as the shaded parts of the cylinder in Figure 7B). However, amide exchange data suggest that the hydrophobic portion of each helix is buried in the micelle since hydrophobic residues V10 and Y13 exchange slower than the hydrophilic residues in the N-terminal helix. The helical distortion around residues 15–17 apparently allows a phase shift to occur that positions nearly all of the hydrophobic residues (and none of the hydrophilic ones) on a single face of the helix. This phase shift is required for both hydrophobic helical segments to be able to favorably interact with the hydrophobic portion of the micelle or membrane. G16 thus very possibly plays an important role in allowing for the helical distortion in this region of the peptide so as to allow the peptide to present a single face of hydrophobic residues to the membrane.

Comparison of the Structure, Dynamics, and Function of Glucagon and Glucagon-like Peptide. Do the X-ray and NMR structures of glucagon and GLP-1 peptide in crystalline and micellar environments provide any biological useful data? Even if the micelle does a good job of mimicking the membrane environment of a cell, the ultimate action of these peptides is on their respective receptor proteins. Thus, GLP-1-(7–36)-NH_2 has been shown to act by binding to a receptor located on the surface of pancreas β-cells (Thorens, 1992). Glucagon binds to a similar receptor. In purely aqueous solution, these short peptides are largely random coils. Even in the membranelike environment of the micelle, these peptides are still quite flexible molecules (although the individual segments of α-helices are relatively rigid). An important caveat must always be raised whether the conformation of the peptides, even on the surface of the membrane (let alone micelle), has any relevance to our understanding of the conformational features of the peptide that are recognized in the receptor-bound state.

Hydrophobic forces are likely responsible for the association of these amphiphilic α-helical peptides to the membrane. Though never unequivocally proved, support for the hydrophobic interactions comes from the observation that many synthetic amphiphilic peptides will form helical structures when in an hydrophobic environment (Bruch & Hoyt, 1992; Karslake et al., 1990). One advantage of this initial anchoring of the peptide to the membrane is that it can diffuse across the surface of the membrane until it meets an appropriate receptor. Diffusion upon the surface of the membrane would allow the peptide to search more quickly in 2D space rather than in the 3D space of the cytosol.

Surprisingly, neither glucagon nor GLP-1 can form a uniform, perfectly amphiphilic helix upon binding to a membrane since the hydrophobic face of the N-terminal portion of the helix is positioned in nearly perfect opposition to the hydrophobic face of the C-terminal segment. The only way that both helical segments can contribute to binding of the peptide to the membrane is to distort the conformation of the residues linking the two hydrophobic helical segments. In GLP-1, glycine-16 will certainly accomplish this because of the helix destabilizing effect of a glycine. In glucagon, residue 16 is a serine, and indeed, in the crystal structure, the peptide is a uniform α-helix extending from residues 6 to 29 (Sasaki et al., 1975). Because the two hydrophobic segments are on opposite faces of the glucagon helix (as modeled in Figure 7B), efficient hydrophobic packing of the individual helices is made possible only by the unusual triangular packing of three helices in the crystal state. The N-terminal hydrophobic face is oriented toward the C-terminal hydrophobic face of a second glucagon molecule while its C-terminal hydrophobic face is oriented toward the N-terminal face of a third helix. In the micelle-bound state, both hydrophobic patches are oriented toward the same face (cf. Figure 7C).

Because Gly-16 in GLP-1 is substituted for a Ser in glucagon, it is likely that it would be more difficult to distort glucagon than GLP-1 into this membrane-binding conformation. Indeed, some photo-CIDNP NMR studies of glucagon bound to vesicles have shown that Y10 and/or Y13 are exposed to solvent while W25 is buried within the membrane (Maurer et al., 1991). This is consistent with our NH exchange data which indicate that the hydrophobic face of the C-terminal helix is significantly more stable or buried more deeply into the micelle than the N-terminal helix (compare the relative

intensities of the V10, S12, and Y13 cross peaks against those of the C-terminal cross peaks in Figure 6A,B). Interestingly, although all mammalian GLP-1's studied have a glycine at position 16, a number of piscine GLP-1's have a Q, N, or K residue substitution (Mojsov et al., 1990).

GLP-1-(7–36)NH_2 binds to its receptor in COS cells at concentrations of 0.5–1 nM. Glucagon can displace bound GLP-1 at a 50% level only at concentrations of 1 μM (Thorens, 1992). The nature of the linking residues between the two helices and the phase shift of the N-terminal helix relative to the C-terminal helix segment may play a role contributing to these differences between glucagn and GLP-1. A related effect has been observed in recognition and processing of a mitochondrial precursor sequence from the precursor protein of rat liver alcohol dehydrogenase (ALDH). The 22-amino-acid signal peptide of the ALDH precursor protein bound to a dodecylphosphocholine micelle has also been shown by 2D NMR to consist of two amphiphilic helical domains separated by a flexible Arg-Gly-Pro linker (Karslake et al., 1990). A signal peptide that is missing these three linker residues was shown to be a single α-helix, and the precursor protein was equally well transported into the mitochondrion (Thornton et al., 1993). However, unlike native ALDH precursor protein, the linker-deleted signal peptide precursor protein could *no longer be processed* after import into mitochondria. The Arg-Gly-Pro deletion is far removed from the cleavage site, suggesting that orientation or relative stability of the amphiphilic α-helix itself may play an important role in proper processing. By removing three residues in the center of the helix, a phase shift of the amphiphilic helix had occurred, moving the first several residues of the mature protein toward the hydrophilic face. Perhaps processing of the precursor protein requires that the first several residues of the mature protein be part of the hydrophobic membrane-associated face of the helix. By moving them toward the hydrophilic face, the proteolytic signal-processing protein is unable to recognize these residues. Alternatively, the NMR data showed that the linker-deleted single helix was more stably bound to the membrane than the helix–linker–helix native sequence. Perhaps the single helix of the linker-deleted signal peptide is *too* stable. Thus, import and processing could require a trade-off in the relative stability and dynamics of various segments of the precursor sequence.

It is not unreasonable to assume that perhaps a portion of the differences between GLP-1, glucagon, and other related peptides resides in the different ways in which they can accommodate the phase shift required to present both N- and C-terminal helical segments toward the membrane surface. These results demonstrate the importance of coupling structural data with the interpretation of biological function.

REFERENCES

Bax, A., & Davis, D. G. (1985) *J. Magn. Reson. 65*, 355–360.

Bösch, C., Brown, L. R., & Wüthrich, K. (1980) *Biochem. Biophys. Acta 603*, 298–312.

Braun, W., Wider, G., Lee, K. H., & Wuthrich, K. (1983) *J. Mol. Biol. 169*, 921–948.

Braunschweiler, L., & Ernst, R. R. (1983) *J. Magn. Reson. 53*, 521–528.

Bruch, M. D., & Hoyt, D. W. (1992) *Biochim. Biophys. Acta 1159*, 81–93.

Clore, G. M., Gronenborn, A. M., Nilges, M., & Ryan, C. A. (1987) *Biochemistry 26*, 8012–8023.

Englander, S. W., & Kallenbach, N. R. (1984) *Q. Rev. Biophys. 19*, 521–655.

Gutniak, M., Ørskov, C., Holst, J. J., Ahrén, B., & Efendć, S. (1992) *N. Engl. J. Med. 326*, 1316.

Hahn, U., & Rüterjans, H. (1985) *Eur. J. Biochem. 152*, 481–491.

Henry, G. D., & Sykes, B. D. (1990) *Biochemistry 29*, 6303–6313.

Henry, G., Weiner, J., & Sykes, B. (1987a) *Biochemistry 26*, 3619–3626.

Henry, G., Weiner, J., & Sykes, B. (1987b) *Biochemistry 26*, 3626–3634.

Hruby, V. J., Krstenansky, J., Gysin, B., Pelton, J. T., Trivedi, D., & McKee, R. L. (1986) *Biopolymers 25*, 135–155.

Karslake, C., Piotto, M. E., Pak, Y. M., Weiner, H., & Gorenstein, D. G. (1990) *Biochemistry 29*, 9872–9878.

Langridge, R., & Ferrin, T. E. (1984) *J. Mol. Graphics 2*, 56.

Maurer, W., Lücke, C., & Rütterjans, H. (1991) *Eur. J. Biochem. 196*, 135–141.

Mojsov, S., Kopczynski, M. G., & Habener, J. F. (1990) *J. Biol. Chem. 265*, 8001–8008.

Molday, R. S., Englander, S. W., & Kallen, R. G. (1972) *Biochemistry 11*, 150–158.

Nikonowicz, E. P., Roongta, V., Jones, C. R., & Gorenstein, D. G. (1989) *Biochemistry 28*, 8714–8725.

Ørskov, C., Bersani, M., Johnsen, A. H., Højrup, P., & Holst, J. J. (1989) *J. Biol. Chem. 264*, 12826–12829.

Piantini, U., Sørenson, O. W., & Ernst, R. R. (1982) *J. Am. Chem. Soc. 104*, 6800–6801.

Rance, M., Sørensen, O. W., Bodenhausen, G., Wagner, G., Ernst, R. R., & Wüthrich, K. (1983) *Biochem. Biophys. Res. Commun. 117*, 479–485.

Roder, H., Wagner, G., & Wüthrich, K. (1985) *Biochemistry 24*, 7396–7407.

Sasaki, K., Dockerill, S., Adamiak, D. A., Tickle, I. J., & Blundell, T. (1975) *Nature 257*, 751–757.

Thorens, B. (1992) *Proc. Natl. Acad. Sci. U.S.A. 89*, 8641–8645.

Thorens, B., & Waeber, G. (1993) *Diabetes 42*, 1219–1225.

Thornton, K., Wang, Y., Weiner, H., & Gorenstein, D. G. (1993) *J. Biol. Chem.* (in press).

Weiner, P. K., & Kollman, P. A. (1981a) *J. Comput. Chem. 2*, 287.

Weiner, P. K., & Kollman, P. A. (1981b) *J. Comput. Chem. 2*, 287–303.

Wishart, D. S., Sykes, B. D., & Richards, F. M. (1992) *Biochemistry 31*, 1647–1651.

Wüthrich, K. (1986) *NMR of Proteins and Nucleic Acids*, Wiley, New York.

Wüthrich, K., Billeter, M., & Braun, W. (1983) *J. Mol. Biol. 169*, 949–961.